

Measurement of an unusually large magnetic octupole moment in ^{45}Sc challenges state-of-the-art nuclear-structure theory

R. P. de Groot,¹ J. Moreno,¹ J. Dobaczewski,^{2,3} I. Moore,¹ M. Reponen,¹ B. K. Sahoo,⁴ and C. Yuan⁵

¹*Department of Physics, University of Jyväskylä, PB 35(YFL) FIN-40351 Jyväskylä, Finland**

²*Department of Physics, University of York, Heslington, York YO10 5DD, United Kingdom*

³*Institute of Theoretical Physics, Faculty of Physics, University of Warsaw, ul. Pasteura 5, PL-02-093 Warsaw, Poland*

⁴*Atomic, Molecular and Optical Physics Division,*

Physical Research Laboratory, Navrangpura, Ahmedabad 380009, India

⁵*Sino-French Institute of Nuclear Engineering and Technology, Sun Yat-Sen University, Zhuhai 519082, China*

(Dated: June 5, 2022)

We measure the hyperfine C -constant of the $3d4s^2\ ^2D_{5/2}$ atomic state in ^{45}Sc : $C = -0.25(12)$ kHz. High-precision atomic calculations of the hyperfine structure of the $3d4s^2\ ^2D_{5/2}$ state and second-order corrections are performed to infer the nuclear magnetic octupole moment $\Omega = 1.6(8)\mu_N b$. With a single valence proton outside of the doubly-magic calcium core, this element is ideally suited for an in-depth study of the many intriguing nuclear structure phenomena observed within the neighboring isotopes of calcium. We compare Ω to shell-model calculations, and find that they cannot reproduce the experimental value of Ω for ^{45}Sc . We furthermore explore the use of Density Functional Theory for evaluating Ω , and obtain values in line with the shell-model calculations. This work provides a crucial step in guiding future measurements of this fundamental quantity on radioactive scandium isotopes and will hopefully motivate a renewed experimental and theoretical interest.

The application of laser spectroscopic techniques to elucidate the subtle perturbations of atomic energy levels due to the nuclear electromagnetic properties has given rise to the study of fundamental nuclear structure, in particular magnetic dipole moments (μ), electric quadrupole moments (Q) and changes in the mean-squared nuclear charge radii $\delta\langle r^2\rangle$. These methods, in combination with modern radioactive ion beam (RIB) facilities, offer a powerful probe of changes in the structure of exotic nuclei. They provide information on nuclear shell evolution, nuclear shapes and sizes, and single-particle correlations which emerge as, for example, local staggering variations in charge radii [1–6]. The majority of the experimental techniques in current use at RIB facilities provide measurements of hyperfine frequency splittings with a precision of 1 - 10 MHz [7]. This limitation restricts the sensitivity to higher order terms in the electromagnetic multipole expansion of the nuclear current densities, as well as to higher order radial moments of the charge density distribution. The progress in the development of higher precision methods along with ongoing development of theoretical tools has the potential to open up a new paradigm in our understanding of the atomic nucleus.

Recently, high-precision isotope shift measurements combined with improved atomic calculations were proposed for a determination of the fourth-order radial moment of the charge density [8], which can in turn be directly linked to the surface thickness of nuclear density [9]. The hyperfine anomaly, only measured for a handful of radioactive isotopes (see e.g. [10–14]), would shed light on the distribution of magnetisation inside the nuclear volume [15, 16]. In addition to the M1 and E2

moments, μ and Q respectively, the M3 magnetic octupole moment Ω is in principle accessible using existing techniques for radioactive isotopes. To our knowledge however, this observable has only been measured for 18 stable isotopes [17–30]. The general features of these values can be understood in terms of the Schwartz limits [31]. However, there are notable exceptions: the recently measured Ω of ^{133}Cs [24] and ^{173}Yb [27] are larger than expected.

The extraction of a higher-order electromagnetic moment from the evaluation of atomic spectra in a nuclear-model independent manner has the potential to provide new insight into the distribution of protons and neutrons within the nuclear volume. Ω is affected by correlations (core polarization and higher order configuration mixing) differently than the magnetic dipole moment, as was highlighted via calculations of the nuclear magnetization distribution of ^{209}Bi [32]. Thus, measurements of Ω may serve to test our understanding of the nucleon-nucleon forces inside the nuclear medium in novel ways. Measurements of Ω may furthermore help to address open questions related to e.g. effective nucleon g -factors and charges. In this Letter, we report on the start of a wide experimental and theoretical effort that will enable an interpretation of measurements of Ω and other higher-order electromagnetic observables on radioactive ions. Our approach is threefold.

Firstly, we demonstrate the feasibility of combining the efficiency of resonance laser ionization spectroscopy (RIS) [4, 33, 34] with the precision of radio-frequency (RF) spectroscopy. The efficiency provided by the RIS method is vital for future applications on radioactive isotopes due to limited production rates of radioactive ion

beams at on-line facilities. The combination with RF spectroscopy offers a dramatic improvement in the precision, by at least three orders of magnitude. We demonstrate this with a high-precision measurement of three nuclear electromagnetic moments of ^{45}Sc , including Ω .

Secondly, we combine these measurements with state-of-the-art atomic-structure calculations to evaluate the sensitivity of the $3d4s^2\ ^2D_{5/2}$ state in neutral scandium to the nuclear octupole moment Ω . We furthermore evaluate the impact of off-diagonal hyperfine structure effects on the extraction of Ω . These calculations are essential to extract Ω from the measurements. We note that the metastable $D_{5/2}$ state is expected to be well-populated in a fast-beam charge exchange reaction [35]. Therefore, radioactive scandium isotopes could be studied using collinear laser-double resonance methods [36, 37] in the future.

Thirdly, with a single proton outside a doubly-magic calcium ($Z = 20$) core, comparison of Ω for a chain of scandium isotopes could help shed light on the many intriguing nuclear structure phenomena observed in the calcium isotopes [3, 38–40]. The proximity to proton- and neutron shell closures makes it possible to perform both shell-model and Density Functional Theory (DFT) calculations. As we seek to eventually examine all existing values of Ω in one consistent framework, with measurements for nuclei scattered throughout the nuclear landscape, developing a reliable global theory for magnetic properties would be highly advantageous. So far, very little is known regarding the overall performance of standard nuclear DFT in describing μ , cf. Refs. [41–43], and nothing is known about the DFT values of Ω . Here, we thus start this investigation with ^{45}Sc . The comparison to nuclear shell-model calculations, which have a more well-established track record in computing both μ and Ω (see e.g. [44]), serves to benchmark these developments.

The value of Ω can be extracted from the first-order shift ($E_F^{(1)}$) in the hyperfine structure interval given by:

$$E_F^{(1)} = A\mathbf{I} \cdot \mathbf{J} + B \frac{3(\mathbf{I} \cdot \mathbf{J})^2 + \frac{3}{2}(\mathbf{I} \cdot \mathbf{J}) - I(I+1)J(J+1)}{2I(2I-1)J(2J-1)} + C \left[\frac{10(\mathbf{I} \cdot \mathbf{J})^3 + 20(\mathbf{I} \cdot \mathbf{J})^2}{I(I-1)(2I-1)J(J-1)(2J-1)} + \frac{2\mathbf{I} \cdot \mathbf{J}\{I(I+1) + J(J+1) - 3N + 3\} - 5N}{I(I-1)(2I-1)J(J-1)(2J-1)} \right], \quad (1)$$

where $\mathbf{I} \cdot \mathbf{J} = \frac{1}{2}[F(F+1) - I(I+1) - J(J+1)]$ and $N = I(I+1)J(J+1)$. In these expressions, I , J and F are the nuclear, atomic, and total angular momentum, while A , B and C are the magnetic dipole (M1), electric quadrupole (E2) and magnetic octupole (M3) hyperfine structure constants, respectively. These are all proportional to their corresponding nuclear moment, in a way which depends on the field distribution of the electrons at the site of the nucleus. Thus, accurate atomic structure calculations of C/Ω have to be performed to extract

Ω from C .

There are three stages in our experiment. First, by tuning a continuous wave (cw) laser into resonance with a transition from one of the hyperfine levels (F) of the atomic ground state into a corresponding hyperfine level of an excited J state, population may be optically pumped. Through de-excitation from the excited state into either another level (F') of the ground-state hyperfine manifold, or into other dark states, the state F is depleted. If RIS is subsequently performed starting from the same F state, a reduced ion count rate is observed. If now, prior to the laser ionization stage, an RF field is tuned into resonance with a $(F, m_F) \rightarrow (F', m_{F'})$ transition, the observed ion count rate again increases. By scanning the frequency of the RF and recording the ion count rate, the hyperfine spacing between the levels F and F' of the ground-state manifold can thus be measured precisely.

We produced an atomic beam of stable scandium by resistively heating a tantalum furnace. Just above the exit orifice of the furnace, up to 15 mW of cw laser light crossed the atom beam orthogonally, in order to optically pump the atoms. This light was produced with a frequency-doubled Sirah Matisse Ti:Sapphire laser, focused to a ~ 1 mm spot above the furnace. The laser was tuned into resonance with the thermally populated $3d4s^2\ ^2D_{5/2}$ state at 168.3371 cm^{-1} , driving an optical transition to the $25\ 014.190\text{ cm}^{-1}\ 3d4s(^3D)4p\ ^2D_{5/2}^o$ state. The atomic beam then passed through a loop of wire through which an RF current was driven, exposing the atoms to an RF field for a few $10\ \mu\text{s}$. The atoms are then collimated and finally orthogonally overlapped with the ionization lasers. A three-step resonant laser ionization scheme was used to ionize the metastable scandium atoms, based on the scheme in [45]. The first step is provided using a $\sim 5\%$ pick-off from the cw laser beam used for the optical pumping stage. The other two steps were produced by pulsed Ti:Sapphire lasers (10 kHz repetition rate), tuned to the $25014.190\text{ cm}^{-1} \rightarrow 46989.493\text{ cm}^{-1}$ transition, and to a broad auto-ionizing state at $\sim 58104\text{ cm}^{-1}$, respectively. Prior to performing any double-resonance measurements, an estimate of the hyperfine constants can be obtained by scanning the frequency of the first laser step, as shown in Fig. 1a.

During the RF scans, the laser wavelength was kept fixed to pumping wavelengths suitable for the different RF lines, and the RF field was introduced and scanned. RF resonances like the examples shown in Fig. 1c were obtained. From the Zeeman splitting observed in wider-range scans (see Fig. 1b), the magnetic field was estimated to be 1.03 G for all but the $(2,0) \rightarrow (1,0)$ transition, where the external field was partially shielded to 80 mG using mu-metal foils. To avoid possible systematics due to e.g. magnetic field inhomogeneities, only the $m_{F'} = 0 \rightarrow m_F = 0$ transitions, magnetically insensitive in first order, were used in the analysis. The final zero-

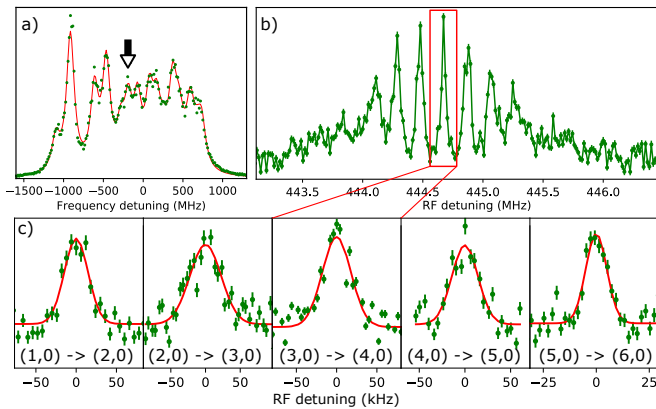


FIG. 1. a) Hyperfine spectrum obtained without the optical pumping and RF steps. b) A wide RF scan, which features several $(F = 4, m_{F=4}) \rightarrow (F = 3, m_{F=3})$ transitions. For this scan, the laser was set to the frequency indicated by the arrow in plot a. c) All five resonances are $m_F = 0 \rightarrow m_F = 0$ lines.

field values for each hyperfine transition are presented in Table I. This table also shows the zero-field corrections. Extracting accurate hyperfine constants requires atomic structure calculations to estimate the second-order shift ($E_F^{(2)}$) due to M1-M1, M1-E2 and E2-E2 interactions.

Line	Line center frequency	B-field corr.	Second-order shift		
			M1-M1	M1-E2	E2-E2
(1, 0) \rightarrow (2, 0)	228 748.2(11)	-0.23	-12.47	1.51	-0.18
(2, 0) \rightarrow (3, 0)	339 116.3(16)	2.31	-2.23	-1.70	0.18
(3, 0) \rightarrow (4, 0)	444 676.0(13)	1.73	3.56	-1.15	-0.16
(4, 0) \rightarrow (5, 0)	543 827.3(18)	0.96	5.79	0.27	-0.05
(5, 0) \rightarrow (6, 0)	634 966.1(5)	0.51	5.34	1.08	0.22

TABLE I. Measured hyperfine resonances $(F, m_F) \rightarrow (F', m_{F'})$ for the $3d4s^2 \ ^2D_{5/2}$ state (shifted to zero B-field using the correction given in the third column). Also given are the zero-field corrections and the second-order shifts. All values are in kHz.

The relativistic coupled-cluster (RCC) theory, known as the gold-standard of many-body theory [46], is used to evaluate C/Ω and the matrix elements involving the second-order hyperfine interaction Hamiltonians. In this work, we expand on earlier calculations [47] presenting A/g_I (with $g_I = \mu/I$), B/Q and C/Ω with a larger set of orbitals, using up to $19s$, $19p$, $19d$, $18f$, $17g$, $16h$ and $15i$ orbitals in the singles- and doubles-excitation approximation in the RCC theory (RCCSD method). Due to limitations in computational resources, we correlate electrons up to g -symmetry orbitals in the singles-, doubles- and triples-excitation approximation in the RCC theory (RCCSDT method). We quote the differences in the results from the RCCSD and RCCSDT methods as ‘+Triples’. Contributions from the Breit and lower-order quantum electrodynamics (QED) interactions are determined using the RCCSD method, and added to the final results as ‘+Breit’ and ‘+QED’, respectively. Con-

tributions due to the Bohr-Weisskopf (BW) effect are estimated in the RCCSD method considering a Fermi-charge distribution within the nucleus and corrections are quoted as ‘+BW’. We also extrapolated contributions from an infinite set of basis functions and present these as ‘Extrapolation’.

The A and B hyperfine constants and the C/Ω values of the $3d4s^2 \ ^2D_{5/2}$ state are tabulated in Table II. To obtain A and B , literature values of the moments were used ($\mu = +4.756487(2) \mu_N$ [48] and $Q = -0.216(9) b$ [17]). Uncertainties are estimated from the neglected higher-level excitations of the RCC theory. Calculations of off-diagonal reduced electronic matrix elements required to estimate the $E_F^{(2)}$, as defined in Ref. [49] as well as in Supplemental Material [50], are also quoted in Table II. We only consider the dominant contributing matrix elements between the $3d4s^2 \ ^2D_{5/2}$ state and the $3d4s^2 \ ^2D_{3/2}$ state. Intermediate results from the zeroth-order calculation using the Dirac-Fock method and the second-order relativistic many-body perturbation theory (RMBPT(2) method) are presented to demonstrate the propagation of electron correlation effects from lower to all-order RCC methods. The final M1-M1, M1-E2 and E2-E2 shifts for each of the lines are given in Tab. I. The final experimental hyperfine constants are summarized in Table III. A non-zero value for C is obtained once second-order corrections are included. Our results agree very well with literature [17], and are an order of magnitude more precise. We find $\Omega = 1.6(8) \mu_N b$. To our knowledge, this is the first determination of Ω for a nucleus with a valence proton in the $f_{7/2}$ shell, thus providing a crucial new constraint for nuclear theory.

Since scandium has a single proton outside of the magic shell of $Z = 20$, the single-particle shell model estimate for Ω [31] could be expected to be fairly good. We find $\Omega_{\text{sm}} = 0.46 \mu_N b$, using $\langle r^2 \rangle^{1/2} = 4.139 \text{ fm}$ (obtained from DFT calculations discussed later). This value is 3.5(17) times smaller than the experimental value. For comparison, for ^{133}Cs the discrepancy is even larger: $\Omega_{\text{exp}} = 0.82(10) \mu_N b$ [24], while $\Omega_{\text{sm}} = 0.14 \mu_N b$ using $\langle r^2 \rangle^{1/2} \approx R = 4.8041(46) \text{ fm}$ [51].

To examine this further, shell-model calculations were performed using different interactions in a $(sd)pf$ -shell model space for ^{45}Sc [52–55], and in the $g_{7/2}sdh_{11/2}$ shell [56–58] for ^{133}Cs . The Ω for both ^{45}Sc and ^{133}Cs is dominated by the proton contribution. In ^{133}Cs , the angular momentum and spin contribution to Ω have the opposite sign and thus largely cancel, while for ^{45}Sc the angular momentum and spin contributions have the same sign. For ^{45}Sc , we obtain values in the range 0.41–0.49 $\mu_N b$ with free g -factors and 0.28–0.35 $\mu_N b$ with a spin-quenching factor of 0.6 for the different shell model calculations. The inclusion of cross-shell excitations from the sd -shell to the pf -shell enhances the correlation beyond the single $f_{7/2}$ proton configuration, which results

TABLE II. Theoretical hyperfine constants of the $3d4s^2\ ^2D_{5/2}$ state. The dominant off-diagonal reduced matrix elements $\langle J' || T_e^{(k)} || J \rangle$ required for the estimation of the second-order corrections to the hyperfine intervals are provided in the last two rows.

	Dirac-Fock	RMBPT(2)	RCCSD	+ Triples	+ QED	+ Breit	+ BW	Extrapolation	Total
A	100.20	93.91	106.62	0.85	0.06	0.27	0.01	0.10	108(2) MHz
B	-32.70	-37.55	-38.04	0.28	-0.01	-0.02	~ 0	0.13	-37.7(5) MHz
C/ Ω	0.78	2.33	-17.09	0.58	~ 0	0.80	~ 0	-0.14	-15.9(2) 10^{-2} kHz/ $(\mu_N\text{ b})$
$\langle 3/2 T_e^{(1)} 5/2 \rangle$	83.52	176.18	145.03	10.15	-0.1	0.61		0.1	156(6) MHz/ μ_N
$\langle 3/2 T_e^{(2)} 5/2 \rangle$	311.27	355.29	376.17	-11.27	0.19	0.48		0.02	366(7) MHz/b

TABLE III. Experimental hyperfine constants and Ω values, without and with the second-order corrections. The last three columns summarize the theoretical results for Ω . Hyperfine constants beyond the octupole term were found to be zero within errors, and are thus not included in the fit.

	Uncorrected		Corrected		Schwartz		Shell Model		DFT
	Ref. [17]	This work	Ref. [17]	This work	$g_s = 1$	$g_s = 0.6$	$g_s = 1$	$g_s = 0.6$	
A [MHz]	109.032(1)	109.0325(1)	109.033(1)	109.0329(1)					
B [MHz]	-37.387(12)	-37.390(1)	-37.373(15)	-37.371(1)					
C [kHz]	1.7(10)	0.06(12)	1.5(12)	-0.25(12)					
Ω [$\mu_N\text{ b}$]	-10.7(63)	-0.4(8)	-9.4(75)	+1.6(8)	0.65	0.46	0.45(4)	0.32(4)	0.245(17)

in small increases in Ω . In contrast to ^{45}Sc , the calculated Ω for ^{133}Cs (using a Hamiltonian to be published soon) is very sensitive to the choice of effective g -factors: $0.02\mu_N\text{ b}$ with free g -factors and $0.16\mu_N\text{ b}$ with a spin-quenching factor of 0.6. All shell-model results thus underestimate the value of Ω for ^{45}Sc and ^{133}Cs . Since Ω for $^{35,37}\text{Cl}$ are well reproduced by shell-model calculations [44] even with free g -factors, strong quenching for ^{45}Sc is not expected.

To check if the large experimental value of Ω can be reproduced by nuclear DFT calculations, we determined values of μ , Q , and Ω for oblate states in ^{45}Sc . We used constrained intrinsic mass quadrupole moments $Q_{20} = \langle 2z^2 - x^2 - y^2 \rangle$ varying between 0 and -1 b , with points at -1 b marked by stars, see Fig. 2. The obtained unpaired mean-field solutions were projected on the $I = 7/2^-$ ground-state angular momentum. Configurations were fixed at $\pi 3^1$ and $\nu 3^4$, where 3^n represents the occupied n lowest oblate orbitals in the $\ell = 3\ f_{7/2}$ shell. No effective charges or effective g -factors were used. Details of calculations performed using the code HFODD (version 2.95j) [59, 60] are collected in the Supplemental Material [50]. For all functionals, the experimental value of the electric quadrupole moment of $Q = -0.216(9)\text{ b}$ is reached near $Q_{20} = -1\text{ b}$ [50].

The calculated values of μ and Ω strongly depend on several input ingredients of the calculation. First, even at $Q_{20} = 0$ these values lie far from the Schmidt and Schwartz [31] single-particle estimates. This can be attributed to a strong quadrupole coupling to the occupied neutron $f_{7/2}$ orbitals, which decreases both μ and Ω . Second, the spin polarization, which acts for the Landau spin-spin terms included, also significantly decreases μ and Ω . The effect of spin polarization also depends on the Skyrme functionals. Third, with increasing in-

trinsic oblate deformation, both μ and Ω increase. The latter effect can be removed by pinning down the intrinsic deformation to the experimental value of Q , see stars in Fig. 2. The shaded area in Fig. 2 covers the range of results given by all starred points, and thus represents a very rough estimate of the averages and rms deviations of the DFT results: $\mu_{\text{DFT}} = +4.74(6)\mu_N$ and $\Omega_{\text{DFT}} = +0.245(17)\mu_N\text{ b}$. The value of Ω_{DFT} is a factor of 6.5(33) smaller than the experimental value. Note that Ω_{DFT} is about twice smaller than the effective Schwartz value, and in reasonable agreement with the shell model value obtained with effective g -factors.

In conclusion, we have measured a large magnetic octupole moment Ω in ^{45}Sc , using high-precision experimental techniques and state-of-the-art atomic calculations. The nuclear-structure interpretation of this new value poses a puzzle: while even the simplest single-particle calculations can successfully describe μ and Q , there appears to be no clear way to interpret the large values of Ω in ^{45}Sc and ^{133}Cs . Further experimental work is thus essential to independently verify our result, and to extend Ω -measurements to other elements. This experimental effort should be matched by accurate atomic structure and nuclear structure calculations. As a next experimental step, we are currently designing and constructing a collinear RIS laser-RF apparatus which we will use to extend measurements to radioactive isotopes. In addition to Sc, candidates for future studies include In [21] and Bi [29]. Finally, we are currently in the process of experimentally verifying the large Ω of ^{173}Yb [27], and are initiating systematic calculations of nuclear magnetic dipole and octupole moments.

RPDG received funding from the European Unions Horizon 2020 research and innovation programme un-

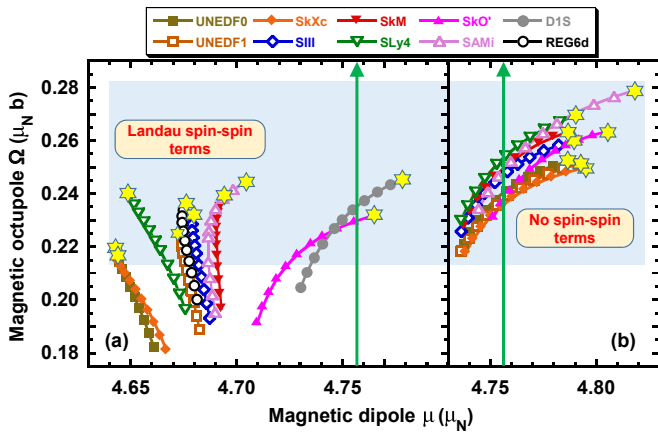


FIG. 2. Values of μ and Ω of the $I = 7/2^-$ angular-momentum-projected ground states of ^{45}Sc . Calculations were performed for eight zero-range Skyrme-type functionals, UNEDF0 [61], UNEDF1 [62], SkXc [63], SIII [64], SkM* [65], SLy4 [66], SAMi [67] and SkO' [68], and for two finite-range functionals, D1S [69] and REG6d.190617 [70]. Panels (a) and (b) show results obtained with Skyrme functionals supplemented by the Landau spin-spin terms or with no spin-spin terms, respectively. Arrows mark the experimental value of μ and point towards the experimental value of Ω , which is outside the scale of the figure

der the Marie Skłodowska-Curie grant agreement No 844829. BKS acknowledges use of Vikram-100 HPC cluster of Physical Research Laboratory, Ahmedabad for atomic calculations. CY acknowledges support of National Natural Science Foundation of China (11775316). This work was supported in part by STFC Grant numbers ST/M006433/1 and ST/P003885/1, and by the Polish National Science Centre under Contract No. 2018/31/B/ST2/02220. We acknowledge the CSC-IT Center for Science Ltd., Finland, for the allocation of computational resources. Fruitful discussions with W. Gins and Á. Koszorus are gratefully acknowledged.

* ruben.p.degroote@jyu.fi

[1] G. Neyens, M. Kowalska, D. Yordanov, K. Blaum, P. Himpe, P. Lievens, S. Mallion, R. Neugart, N. Vermeulen, Y. Utsuno, *et al.*, Phys. Rev. Lett. **94**, 022501 (2005).
 [2] K. Flanagan, P. Vingerhoets, M. Avgoulea, J. Billowes, M. Bissell, K. Blaum, B. Cheal, M. De Rydt, V. Fedosseev, D. Forest, *et al.*, Phys. Rev. Lett. **103**, 142501 (2009).
 [3] R. G. Ruiz, M. Bissell, K. Blaum, A. Ekström, N. Frömmgen, G. Hagen, M. Hammen, K. Hebel, J. Holt, G. Jansen, *et al.*, Nat. Phys. **12**, 594 (2016).
 [4] B. Marsh, T. D. Goodacre, S. Sels, Y. Tsunoda, B. Andel, A. Andreyev, N. Althubiti, D. Atanasov, A. Barzakh, J. Billowes, *et al.*, Nat. Phys. **14**, 1163 (2018).

[5] Y. Ichikawa, Bulletin of the American Physical Society **63** (2018).
 [6] A. J. Miller, K. Minamisono, A. Klose, D. Garand, C. Kujawa, J. Lantis, Y. Liu, B. Maaß, P. Mantica, W. Nazarewicz, *et al.*, Nat. Phys. **15**, 432 (2019).
 [7] P. Campbell, I. Moore, and M. Pearson, Prog. Part. Nucl. Phys. **86**, 127 (2016).
 [8] A. Papoulia, B. G. Carlsson, and J. Ekman, Phys. Rev. A **94**, 042502 (2016).
 [9] P.-G. Reinhard, W. Nazarewicz, and R. G. Ruiz, Phys. Rev. C **101**, 021301 (2020).
 [10] J. Grossman, L. Orozco, M. Pearson, J. Simsarian, G. Sprouse, and W. Zhao, Phys. Rev. Lett. **83**, 935 (1999).
 [11] A. Takamine, M. Wada, K. Okada, T. Sonoda, P. Schury, T. Nakamura, Y. Kanai, T. Kubo, I. Katayama, S. Ohtani, H. Wollnik, and H. A. Schuessler, Phys. Rev. Lett. **112**, 162502 (2014).
 [12] J. Papuga, M. L. Bissell, K. Kreim, C. Barbieri, K. Blaum, M. De Rydt, T. Duguet, R. F. Garcia Ruiz, H. Heylen, M. Kowalska, R. Neugart, G. Neyens, W. Nörtershäuser, M. M. Rajabali, R. Sánchez, N. Smirnova, V. Somà, and D. T. Yordanov, Phys. Rev. C **90**, 034321 (2014).
 [13] S. Schmidt, J. Billowes, M. Bissell, K. Blaum, R. G. Ruiz, H. Heylen, S. Malbrunot-Ettenauer, G. Neyens, W. Nörtershäuser, G. Plunien, S. Sailer, V. Shabaev, L. Skripnikov, I. Tupitsyn, A. Volotka, and X. Yang, Phys. Lett. B **779**, 324 (2018).
 [14] J. R. Persson, Atoms **8** (2020), 10.3390/atoms8010005.
 [15] H. H. Stroke, H. Duong, and J. Pinard, Hyperfine Interact. **129**, 319 (2000).
 [16] F. Karpeshin and M. Trzhaskovskaya, Nucl. Phys. A **941**, 66 (2015).
 [17] W. J. Childs, Phys. Rev. A **4**, 1767 (1971).
 [18] R. T. Daly and J. H. Holloway, Phys. Rev. **96**, 539 (1954).
 [19] H. H. Brown and J. G. King, Phys. Rev. **142**, 53 (1966).
 [20] W. L. Faust and L. Y. Chow Chiu, Phys. Rev. **129**, 1214 (1963).
 [21] T. G. Eck and P. Kusch, Phys. Rev. **106**, 958 (1957).
 [22] V. Jaccarino, J. G. King, R. A. Satten, and H. H. Stroke, Phys. Rev. **94**, 1798 (1954).
 [23] W. L. Faust and M. N. McDermott, Phys. Rev. **123**, 198 (1961).
 [24] V. Gerginov, A. Derevianko, and C. E. Tanner, Phys. Rev. Lett. **91**, 072501 (2003).
 [25] N. C. Lewty, B. L. Chuah, R. Cazan, B. K. Sahoo, and M. D. Barrett, Opt. Express **20**, 21379 (2012).
 [26] P. J. Unsworth, J. Phys. B **2**, 122 (1969).
 [27] A. K. Singh, D. Angom, and V. Natarajan, Phys. Rev. A **87**, 012512 (2013).
 [28] M. N. McDermott and W. L. Lichten, Phys. Rev. **119**, 134 (1960).
 [29] D. A. Landman and A. Lurio, Phys. Rev. A **1**, 1330 (1970).
 [30] G. H. Fuller, J. Phys. Chem. Ref. Data **5**, 835 (1976).
 [31] C. Schwartz, Phys. Rev. **97**, 380 (1955).
 [32] R. Sen'kov and V. Dmitriev, Nucl. Phys. A **706**, 351 (2002).
 [33] R. Ferrer, A. Barzakh, B. Bastin, R. Beerwerth, M. Block, P. Creemers, H. Grawe, R. de Groote, P. Delahaye, X. Fléchar, *et al.*, Nat. Commun. **8**, 1 (2017).
 [34] R. de Groote, J. Billowes, C. Binnersley, M. Bissell, T. Cocolios, T. D. Goodacre, G. Farooq-Smith, D. Fe-

- dorov, K. Flanagan, S. Franchoo, et al., arXiv preprint arXiv:1911.08765 (2019).
- [35] A. Vernon, J. Billowes, C. Binnersley, M. Bissell, T. Cocolios, G. Farooq-Smith, K. Flanagan, R. G. Ruiz, W. Gins, R. de Groote, . Koszors, K. Lynch, G. Neyens, C. Ricketts, K. Wendt, S. Wilkins, and X. Yang, *Spectrochimica Acta Part B: Atomic Spectroscopy* **153**, 61 (2019).
- [36] U. Nielsen, O. Poulsen, P. Thorsen, and H. Crosswhite, *Phys. Rev. Lett.* **51**, 1749 (1983).
- [37] W. Childs, *Physics reports* **211**, 113 (1992).
- [38] D. Steppenbeck, S. Takeuchi, N. Aoi, P. Doornenbal, M. Matsushita, H. Wang, H. Baba, N. Fukuda, S. Go, M. Honma, et al., *Nature* **502**, 207 (2013).
- [39] F. Wienholtz, D. Beck, K. Blaum, C. Borgmann, M. Breitenfeldt, R. B. Cakirli, S. George, F. Herfurth, J. Holt, M. Kowalska, et al., *Nature* **498**, 346 (2013).
- [40] M. Tanaka, M. Takechi, A. Homma, M. Fukuda, D. Nishimura, T. Suzuki, Y. Tanaka, T. Moriguchi, D. Ahn, A. Aimaganbetov, et al., arXiv preprint arXiv:1911.05262 (2019).
- [41] O. I. Achakovskiy, S. P. Kamerzhiev, E. E. Saperstein, and S. V. Tolokonnikov, *The European Physical Journal A* **50**, 6 (2014).
- [42] L. Bonneau, N. Minkov, D. D. Duc, P. Quentin, and J. Bartel, *Phys. Rev. C* **91**, 054307 (2015).
- [43] M. Borrajo and J. L. Egido, *Physics Letters B* **764**, 328 (2017).
- [44] B. A. Brown, W. Chung, and B. Wildenthal, *Phys. Rev. C* **22**, 774 (1980).
- [45] S. Raeder, M. Dombbsky, H. Heggen, J. Lassen, T. Quenzel, M. Sjödin, A. Teigelhöfer, and K. Wendt, *Hyperfine Interact.* **216**, 33 (2013).
- [46] I. Shavitt and R. J. Bartlett, *Many-body methods in chemistry and physics: MBPT and coupled cluster methods* (Cambridge university press, 2009).
- [47] B. K. Sahoo, T. Beier, B. Das, R. Chaudhuri, and D. Mukherjee, *J. Phys. B* **38**, 4379 (2005).
- [48] O. Lutz, *Physics Letters A* **29**, 58 (1969).
- [49] B. K. Sahoo, *Phys. Rev. A* **92**, 052506 (2015).
- [50] See Supplemental Material at [URL will be inserted by publisher] for details related to hyperfine structure constants and to numerical DFT calculations as well as for plots and numerical values of calculated energies, magnetic octupole moments, and magnetic dipole moments, which includes Refs. [71–77].
- [51] I. Angeli and K. Marinova, *At. Data Nucl. Data Tables* **99**, 69 (2013).
- [52] M. Honma, T. Otsuka, B. A. Brown, and T. Mizusaki, *Phys. Rev. C* **65**, 061301 (2002).
- [53] M. Honma, T. Otsuka, B. A. Brown, and T. Mizusaki, *Eur. Phys. J. A* **25**, 499 (2005).
- [54] A. Abzouzi, E. Caurier, and A. P. Zuker, *Phys. Rev. Lett.* **66**, 1134 (1991).
- [55] A. Poves, J. Snchez-Solano, E. Caurier, and F. Nowacki, *Nucl. Phys. A* **694**, 157 (2001).
- [56] Y. Utsuno, T. Otsuka, T. Mizusaki, and M. Honma, *Phys. Rev. C* **60**, 054315 (1999).
- [57] Y. Utsuno, T. Otsuka, B. A. Brown, M. Honma, T. Mizusaki, and N. Shimizu, *Phys. Rev. C* **86**, 051301 (2012).
- [58] F. Nowacki and A. Poves, *Phys. Rev. C* **79**, 014310 (2009).
- [59] N. Schunck, J. Dobaczewski, W. Satuła, P. Bączyk, J. Dudek, Y. Gao, M. Konieczka, K. Sato, Y. Shi, X. Wang, and T. Werner, *Comp. Phys. Commun.* **216**, 145 (2017).
- [60] J. Dobaczewski, (2020), *et al.*, to be published.
- [61] M. Kortelainen, T. Lesinski, J. Moré, W. Nazarewicz, J. Sarich, N. Schunck, M. V. Stoitsov, and S. Wild, *Phys. Rev. C* **82**, 024313 (2010).
- [62] M. Kortelainen, J. McDonnell, W. Nazarewicz, P.-G. Reinhard, J. Sarich, N. Schunck, M. V. Stoitsov, and S. M. Wild, *Phys. Rev. C* **85**, 024304 (2012).
- [63] B. A. Brown, *Phys. Rev. C* **58**, 220 (1998).
- [64] M. Beiner, H. Flocard, N. V. Giai, and P. Quentin, *Nuclear Physics A* **238**, 29 (1975).
- [65] J. Bartel, P. Quentin, M. Brack, C. Guet, and H.-B. Håkansson, *Nuclear Physics A* **386**, 79 (1982).
- [66] E. Chabanat, P. Bonche, P. Haensel, J. Meyer, and R. Schaeffer, *Nuclear Physics A* **635**, 231 (1998).
- [67] X. Roca-Maza, G. Colò, and H. Sagawa, *Phys. Rev. C* **86**, 031306 (2012).
- [68] P.-G. Reinhard, *Nucl. Phys. A* **649**, 305c (1999).
- [69] J. Berger, M. Girod, and D. Gogny, *Computer Physics Communications* **63**, 365 (1991).
- [70] K. Bennaceur, J. Dobaczewski, T. Haverinen, and M. Kortelainen, arXiv:2003.10990 (2020).
- [71] J. Sheikh, J. Dobaczewski, P. Ring, L. Robledo, and C. Yannouleas, arxiv:1901.06992 (2019).
- [72] Y. Engel, D. Brink, K. Goeke, S. Krieger, and D. Vautherin, *Nuclear Physics A* **249**, 215 (1975).
- [73] E. Perlińska, S. G. Rohoziński, J. Dobaczewski, and W. Nazarewicz, *Phys. Rev. C* **69**, 014316 (2004).
- [74] J. Negele, *Effective Interactions and Operators in Nuclei*, edited by B. Barrett, *Lecture Notes in Physics*, Vol. 40 (Springer-Verlag Berlin Heidelberg, 1975) p. 270.
- [75] M. Bender, J. Dobaczewski, J. Engel, and W. Nazarewicz, *Phys. Rev. C* **65**, 054322 (2002).
- [76] J. Dobaczewski and P. Olbratowski, *Computer Physics Communications* **158**, 158 (2004).
- [77] M. Bender, (2020), *et al.*, to be published.